ISSN 1946-7664. MCFNS 2015
Vol. 7, Issue 2, pp. 66–80
Mathematical and Computational Forestry & Natural-Resource Sciences

AVAILABLE ONLINE AT HTTP://MCFNS.COM

Submitted: Sep. 10, 2015
Accepted: Sep. 27, 2015
Published: Sep. 30, 2015
Last Correction: Oct. 1, 2015

EVALUATING DIFFERENT MODELS TO PREDICT BIOMASS INCREMENT FROM MULTI-TEMPORAL LIDAR SAMPLING AND REMEASURED FIELD INVENTORY DATA IN SOUTH-CENTRAL ALASKA

H. Temesgen[1], J. Strunk[2], H.-E. Andersen[3], J. Flewelling[4]

[1] *Dept. For. Eng., Resources and Management, Oregon State University, Corvallis, OR, USA*
[2] *Washington State Department of Natural Resources, Seattle, WA, USA*
[3] *USDA Forest Service, Pacific Northwest Research Station, Seattle, WA, USA*
[4] *Seattle Biometrics, Seattle, WA, USA*

Abstract. We evaluated two sets of equations for their predictive abilities for estimating biomass increment using successively acquired airborne lidar and ground data collected on western lowlands of the Kenai Peninsula in south-central Alaska. The first set included three base equations for estimating biomass increment as a function of lidar metrics, and the remaining equations enhanced the three base equations by considering the hierarchical structure of the data.

It is shown that the mixed effect framework substantially improved the accuracy and precision of biomass increment prediction over a model without the plot effects that assume the observations are independent for the area covered by two lidar acquisitions, 5 years apart from one another. On the average, root mean square error values were reduced by 19.8% by using a plot-level random coefficient model that account for the impacts of site (biophysical factors) on biomass increment on the western Kenai Peninsula.

Mixed effect models are effective statistical tools, but their effective application requires some sample growth data. As such, we recommend two models for estimating biomass increment on the Kenai Peninsula. If a subsample of ground data is available to predict the plot random intercept, the enhanced model is suggested. In the absence of ground data, an alternative model a model without the plot effects is suggested. Model coefficients are documented to facilitate development of a multi-part estimation strategy which includes both decay and increment.

Keywords: LiDAR, Mixed model, Alaska, Pacific Northwest

1 Introduction

Information on forest biomass and its increment is increasingly being used to guide the location of new biomass processing plants (Andersen et al. 2011), quantify wildlife habitat capability (Hyde et al. 2006), model carbon balance and storage (Gough et al. 2008), determine the components of forest fuels (Andersen et al. 2005), predict the effect of climate change on forest productivity (Latta et al. 2009), and develop forest restoration thinning and fire hazard management plans (Edmons et al. 2000, Temesgen et al. 2007) and greenhouse gas policy analysis (Baker et al. 2010).

Performing field measurement to quantify biomass increment is time- and labor- intensive. Yet, there is a need for accurate and up-to-date information on biomass increment for sustainable forest management. Conventionally, biomass increment models have used only ground attributes as predictor variables. Recent studies, however, indicate that lidar may offer a quicker and more cost-effective method of data collection with the potential not only to provide predictions for current status but

also biomass increment (Bollandsås *et al.* 2013, Hudak *et al.* 2012, Meyer *et al.* 2013, and Næsset *et al.* 2013).

The use of small-footprint lidar for estimation of forest yield variables has been well-established in the literature. Much of the research into the use of lidar for forest applications has assessed variables such as tree height, volume and biomass. Many studies have used regression analysis to relate lidar-derived metrics to a large number of additional field-based inventory variables including basal area, mean diameter, dominant height, stem density, and vegetation cover (Means et al, 2000; Naesset 2002, Goerndt et al. 2010). Most studies have found strong correlation between lidar derived variables and the inventory parameters obtained from ground-based measurements (Nelson et al, 1988; Nilsson, 1996; Næsset and Bjerknes, 2001; Næsset and Økland, 2002; Donoghue and Watt, 2006). However, few studies have attempted to quantify biomass increment using repeated lidar measurements (Bollandsås *et al.* 2013, Hudak *et al.* 2012, Meyer *et al.* 2013, Næsset *et al.* 2013, and McRoberts *et al.* 2014).

Estimating biomass increment is a complicated task with the potential for large errors where model errors could be larger than the predicted increment (Yu et al 2004). While Yu et al (2006) reported strong correlations (0.68) between selected lidar metrics and stand growth, Næsset and Gobakken (2005) reported a weak correlation between these variables, and their comparison with field data suggested increment predictions using lidar had limited accuracy and precision. Common findings from both these studies are that biomass increment predictions are extremely variable and prediction accuracy depends on the fitting techniques used.

Estimation of biomass increment becomes even more problematic when one considers the spatial variability over the landscape. Methods used for considering wide variation and the hierarchical structure of data include mixed effects models and repeated measure analysis. Discussions concerning the effect of data structure on the predictive abilities of biomass increment are infrequent in the literature. Comparison across varying vegetation type and ecological regions were undertaken by Breidenbach *et al* (2007, 2008). Despite the growing research interest in change estimation, detailed analyses that quantify the gains obtained by using lidar metrics and mixed effect models are lacking. Also lacking are analyses that examine the ability, efficiency and suitability of using specific lidar metrics in predicting biomass increment (ΔAGB) and models forms (Bollandsås *et al.* 2013, Hudak *et al.* 2012, Meyer *et al.* 2013, Næsset *et al.* 2013, McRoberts *et al.* 2014).

The forests of interior Alaska are vast, covering approximately 56 million hectares (17% of the US forest land). These forests are characterized by mostly low productivity, inaccessibility, and extremes in both topography and temperature, and are therefore very expensive to inventory and monitor effectively (van Hees 2005). These and other factors have contributed to the lack of ground inventory data in interior Alaska. The emergence of a new generation of advanced remote sensing technologies, such as airborne lidar, which is capable of directly measuring three-dimensional forest structure, has the potential to decrease the number of field plots required to inventory remote regions. The FIA program of the USDA Forest Service Pacific Northwest Research Station has initiated a research project to evaluate how lidar can be used to augment a limited sample of FIA ground plot data. Kenai Peninsula was selected for this project as its vegetation and forest resource types are similar to interior Alaska's forest types which are dominated by white spruce (*Picea glauca* (Moench) Voss), black spruce (*P. mariana* (Mill.) B.S.P.), and paper birch (*Betula papyrifera* Marsh) to those common in the mountainous south-coastal regions (Sitka spruce [*Picea sitchensis* (Bong.) Carr.] and mountain hemlock (*Tsuga mertensiana* (Bong.) Carr.).

The relationship between biomass and lidar metrics varies by stand (Naesset *et al.* 2004, Naesset and Gobakken 2005, Breidenbach *et al* 2007, Goerndt *et al.* 2010), indicating the need for varying parameters among stands. Mixed-model approaches formally incorporate the between-stand variability of biomass-lidar metrics relationships into the model. Estimation of biomass using nonlinear mixed-effects models has been previously reported by Breidenbach *et al* (2007, 2008), but no published work has applied mixed effect model for estimating ΔAGB for Alaskan forests.

The objectives of this study were to: 1) identify and examine selected methods for estimating biomass increment using repeatedly measured lidar and ground data; 2) examine the performance of selected models for estimating biomass increment in Alaskan forests; and 3) examine the potential use of mixed effect models to predict biomass increment.

2 Methods

2.1 Study Area The study was conducted on Kenai Peninsula**,** Alaska (Figure 1). The western lowlands of the Kenai cover approximately 775,000 hectares of forestland. Data for this study were obtained from Forest Inventory and Analysis (FIA) databases for coastal Alaska forests. The FIA databases are part of the national inventory of forests for the United States (Roesch and Reams 1999 and Czaplewski 1999). A tessellation of hexagons, each approximately 2400 hectares in size, is superimposed across the nation, one field plot randomly located within each hexagon. Approximately the same

number of plots is measured each year, and each plot has the same probability of selection. Each field plot is composed of four subplots, with each subplot composed of three nested fixed-radius areas used to sample trees of different sizes (Figure 2). Forested areas that are distinguished by structure, management history, or forest type, are identified as unique units on the plot and correspond to stands of at least 0.4047 hectare in size.

This study is part of a larger project aimed at examining the potential use of lidar to inventory and monitor coastal Alaska forests. Because one of the main objectives of this preliminary study was to evaluate the predictive performance of ΔAGB equations as a function of successive lidar measures, only ground plots that showed increments were included. Accordingly, our 2004 and 2009 FIA data set for Kenai Peninsula contained 22 sample clusters (plots) and 54 subplots that covered a wide array of stand densities and productivity gradients, with basal area ranging from 2.2 to 46.5 m^2/ha; number of tree/ha from 60 to 1190; and elevation from 30.5 to 457.2 m (Table 1).

Table 1: Minimum (Min), average (Mean), maximum (Max), and standard deviation (SD) of selected stand attributes of the data used in the study.

Attribute	Min	Mean	Max	SD
Elevation (m)	30.5	151.8	457.2	10.0
Slope (%)	0.0	5.0	35.0	1.0
Site index (m)	27.0	60.4	85.0	13.3

The ground data used in this study were collected during two measurement periods. Data from the first (early) measurement period were collected between 1999 and 2004 when FIA was still organized as a periodic inventory. Data for the subsequent measurement period (late), from 2004 to 2009, were collected after the transition from periodic to annual inventories by FIA. The re-measurement interval for these plots was not, however, guaranteed to be 5 years. Some of the plots were re-measured after a single year, and some of the plots were re-measured after up to 10 years. For biomass increment, this required normalizing by the number of years between re-measurements. We summarized ground attributes at the sub-plot level from tree records in the databases for the respective periodic and annual inventories. Biomass increment (kg/ha) was calculated as the change in biomass for trees measured during both measurement periods. This means that changes due to mortality and ingrowth were omitted. Due to lack of long term data, no attempt was made to account for structural changes which might affect to tree growth, or mortality (Kenai Peninsula has experienced a beetle epidemic).

Tree biomass was estimated using equations developed for a variety of tree species in Alaska (Yarie et al. 2007). The equations were applied to the trees measured on each plot to obtain a plot-level estimate of above-ground tree biomass. The following ground variables were extracted.

- **Y4 and Y9:** biomass kg for measurement periods ending in 2004 and 2009, respectively.
- **ΔAGB:** 5-year prediction biomass increment in kg/ha for trees measured in both the early and late inventories.

To obtain precise plot coordinates, survey-grade GPS with differential post-processing was used to geo-reference sub-plots (Andersen et al. 2009).

Lidar data

We used two leaf-off airborne laser scanning surveys datasets acquired over the Kenai Peninsula in 2004 and 2009 for this study. Both datasets were collected using small-footprint, discrete-return lidar systems that recorded a target density of 4 pulses /m^2returns. The data were processed to create subplot-level lidar-derived products using Fusion 2.0 (McGaughey et al. 2004). Over 20 lidar-derived variables were evaluated as potential predictors. We selected a number of lidar metrics for examination of relationships to biomass increment based on the strength of their relationship to biomass and biomass increment. The selected predictor variables include lidar canopy height (LCH), percent canopy cover (PCVR), coefficient of variation of lidar canopy height (LCHCV), and differences between successive percent canopy cover values (ΔPCVR).

- **LCH604 and LCH609:** the 60th percentile of all returns lidar canopy height in 2004 and 2009, respectively.
- **LCH904 and LCH909:** the 90th percentile of all returns lidar canopy height in 2004 and 2009, respectively.
- **PCVR4 and PCVR9:** Percent of all-returns lidar heights above 1 meter for the 2004 and 2009 data.
- **LCHCV4 and LCHCV9:** Coefficient of variation (%) of all-returns lidar data in 2004 and 2009.
- **ΔLCH30, ΔLCH60, and ΔLCH90:** Difference in the 30^{th},60^{th}, and 90^{th} percentile of all-returns lidar heights between 2004 and 2009, respectively.

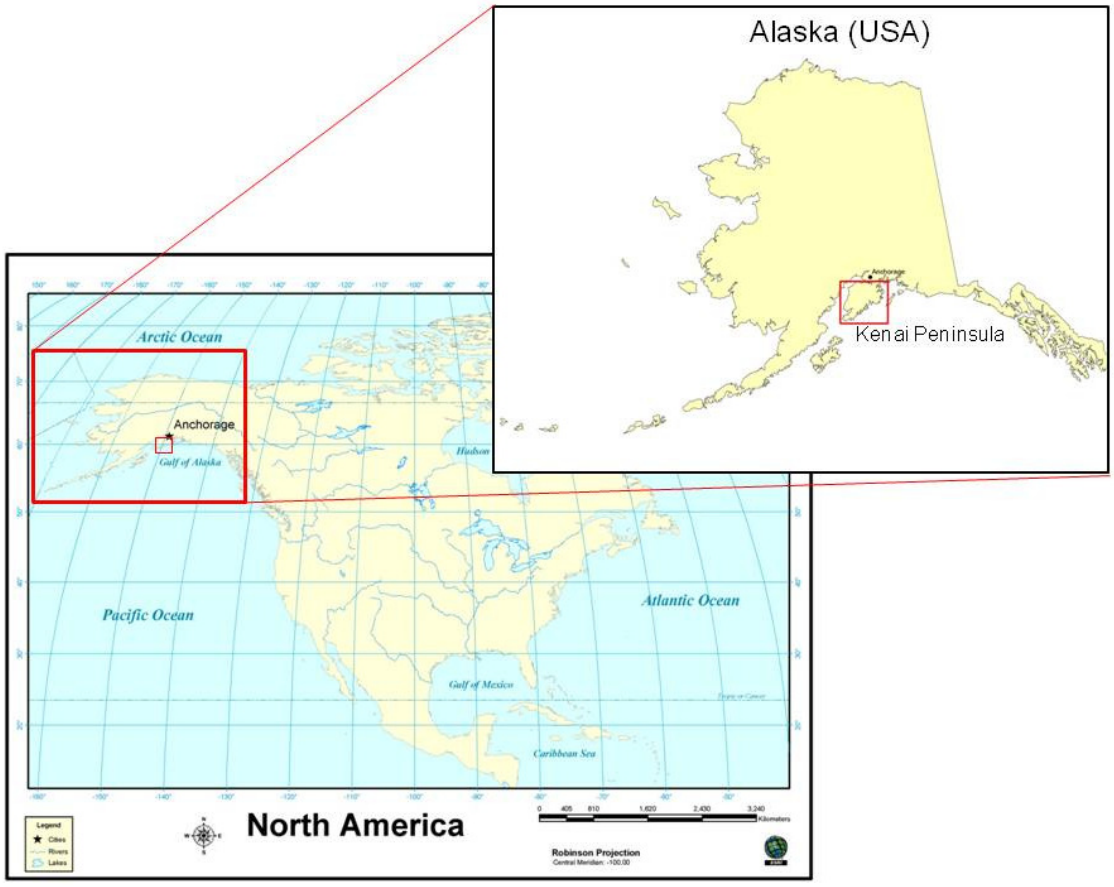

Figure 1: The Kenai Peninsula study site.

- **ΔPCVR:** Differences in coefficients of variation for all-returns lidar heights between 2004 and 2009.

For all base models, explanatory variables that did not contribute significantly (at the 0.05 level) towards explaining variation were dropped from models.

2.2 Data summary The values of AGB ranged from 1929.0 to 213,328.0 kg/ha and 1458.0 to 202,556.0 kg/ha with coefficient of variation of 88.6 and 93.0% in 2004 and 2009, respectively. The values of ΔAGB ranged from 115 to 23,227 kg/ha with coefficient of variation 96.1% (Table 2).

The data indicated that the spread of the ground and lidar attributes have not significantly changed between the two measurement periods. Over five year period, ΔAGB ranged from 115 to 23,227 kg/ha, while the differences ΔLCH90 and ΔPCVR ranged from -1.63 to 1.88 and -0.19 to 25.3%, respectively (Table 2).

The lidar metrics were derived separately for each subplot. The range and variability of the lidar metrics was not remarkably different during the two measurement periods. The 90^{th} percentile lidar canopy height ranged from 5.1 to 19.3 m in 2004, while in 2009 it ranged from 5.0 and 19.0 m. Percent canopy cover ranged from 5.2 to 42.9% and from 10.5 to 64.1% in 2004 and 2009, respectively. The coefficients of variation for the 60^{th} and 90^{th} percentile lidar canopy height were 42.6 and 32.3% and 45.7 and 24.1% in 2004 and 2009, respectively. The coefficients of variation for PCVR were 24.1% and 33.9% in 2004 and 2009, respectively (Table 2).

2.3 Data Analysis The Pearson correlation coefficients were used to quantify the relationships between ΔAGB and selected lidar metrics. Graphical approaches were also used to indicate relationships between ΔAGB and selected lidar metrics in coastal Alaska forests. Following these exploratory analyses, we selected variables that minimized the mean-square-error (MSE) and average deviation (bias) while keeping the model as simple as possible (i.e., minimum number of predictors) to prevent model over-fitting.

In this study, two sets of models were evaluated. Each of the models in the first set has estimators for

Table 2: Summary of selected attributes: minimum (Min), maximum (Max), and standard deviation (Std) (n= 54 subplots).

	2009				2004			
Attribute	Min	Mean	Max	Std	Min	Mean	Max	Std
Biomass(kg/ha)	1,929.0	69,857.0	213,328.0	60,507.5	1,458.0	63,625.0	202,556.0	59,162.0
	Lidar canopy height (m)							
30th percentile	2.3	5.4	12.5	2.4	2.0	5.5	12.2	2.6
60th percentile	3.3	8.2	16.1	3.5	3.0	8.3	15.6	3.8
90th percentile	5.1	11.8	19.3	4.2	5.0	11.5	19.0	4.3
Percent canopy cover	5.2	26.9	42.9	9.5	10.5	39.5	64.1	13.4
Difference								
Biomass increment (kg/ha)	115.0	6,232.0	23,227.0	5,986.1				
	Lidar canopy height (m)							
30th percentile	-0.8	0.1	1.9	0.5				
60th percentile	-1.3	0.1	2.9	0.7				
90th percentile	-1.6	-0.14	1.9	0.4				
Percent canopy cover	-0.2	13.4	25.9	6.6				

biomass at two points in time; increment is estimated as the difference. The second set of models (4 through 6) is fit assuming a mixed-model error structure; only one of these (model 4) also estimates biomass at both points in time. For all models, explanatory variables that did not contribute significantly (at the 0.05 level) towards explaining variation were dropped from models.

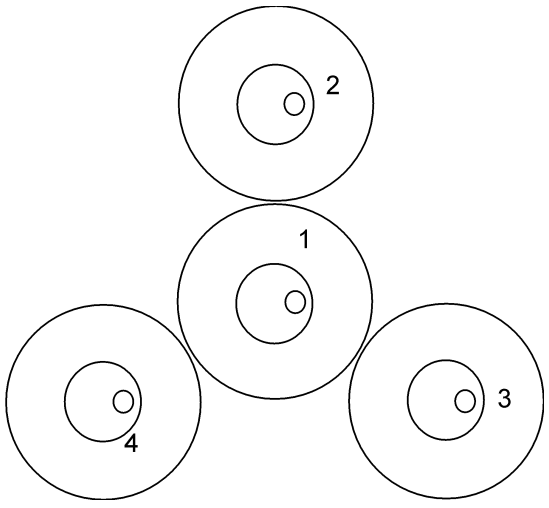

Figure 2: Forest Inventory and Analysis (FIA) plot design, illustrating a single plot, composed of four subplots in a predetermined geometric arrangement. Each subplot is composed of three fixed-radius areas used to sample trees of different sizes. The two larger radii plots (36.6 m and 17.95 m) are concentric, and the small radius plot (2.07 m) is not, (Figure not drawn to scale).

2.4 Modeling Approach Models 1 through 3 are nonlinear models with different lidar metrics and prediction strategies, and assume the mean function is plot invariant with constant residual variance. Models 4 through 6 explicitly incorporate the clustered structure of the sample through random coefficients.

Model 1: Using differences between the 2009 and 2004 lidar-derived biomass predictions

Biomass was regressed against selected lidar attributes to predict its values based on lidar attributes acquired in 2004 (Y4) and 2009 (Y9). ΔAGB was estimated as the difference between the 2009 and 2004 predictions.

$$Y4_{ij} = e^{\beta_0+\beta_1 LCH904_{ij}+\beta_2 PCVR4_{ij}} + \varepsilon_{ij} \quad (1)$$

$$Y9_{ij} = e^{\beta_0+\beta_1 LCH909_{ij}+\beta_2 PCVR9_{ij}} + \varepsilon_{ij} \quad (2)$$

$$\widehat{\Delta AGB}_{ij} = \hat{Y}9_{ij} - \hat{Y}4_{ij} \quad (3)$$

Where:

- n and m denote the number of plots and subplots respectively;
- i refers to plot, $i = 1, \ldots, n$; and j indicates subplots; $j = 1, \ldots, m_i$;
- β_0, β_1; and β_2 are parameters to be estimated;

- $\Delta\widehat{AGB}_{ij}$ is 5-year prediction biomass increment;
- ε_{ij} is an error term, assumed to be independent between observations, such that $\varepsilon_{ij} \sim N\left(0, \sigma_{\varepsilon}^2\right)$;
- LCH904, LCH909, PCVR4, and PCVR9 have been defined earlier; and
- $\hat{Y}9_{ij}$ and $\hat{Y}4_{ij}$ biomass (kg) predictions in 2009 and in 2004.

Model 2: Estimating ΔAGB using differences in lidar attributes

In this approach, differences between selected lidar metrics were calculated by subtracting their 2009 values from their 2004 values (e.g., LCH309 – LCH304). We estimated ΔAGB for each subplot using these differences.

$$\Delta\widehat{AGB}_{ij} = e^{\beta_0+\beta_1\Delta LCH30_{ij}+\beta_2\Delta PCVR_{ij}} + \varepsilon_{ij} \qquad (4)$$

Where:

- $\Delta\widehat{AGB}_{ij}\Delta LCH30$ and $\Delta PCVR$ are the differences in the 30^{th} percentile lidar canopy height (m) and percent canopy cover returns between the 2009 and 2004 lidar acquisitions;
- $\Delta\widehat{AGB}_{ij}$ is predicted 5-year prediction biomass increment;
- and all other symbols are as previously defined.

Model 3: Using differences derived from successive lidar based biomass predictions In this approach, ΔAGB is estimated using successive lidar-based biomass predictions that are adjusted with ordinary least squares (OLS) correction (Draper and Smith 1998, p. 225).

$$\Delta\widehat{AGB}_{ij} = \beta_0 + \beta_1\left(\hat{Y}9_{ij} - \hat{Y}4_{ij}\right) + \varepsilon_{ij} \qquad (5)$$

Where:

- β is the vector of average model parameters;
- $\hat{Y}9_{ij}$ and $\hat{Y}4_{ij}$ are estimated biomass (kg) in 2009 and 2004 using Equations 1 and 2;
- and all other symbols are as previously defined.

Mixed model analysis Mixed model approaches can formally incorporate the within-plot variability of biomass-lidar metrics relationship into the model. Gregoire (1987) asserted that plot random effects account for influences due to site and related variables such as drainage and productivity. Accordingly, we considered the hierarchical structure of the data under the base models (Models 1 through 3), and examined the roles of mixed effects models (MEM) in estimating ΔAGB.

The nonlinear mixed model can be motivated as a hierarchical model (Pinheiro and Bates 2000). Suppose we observe biomass increment and coinciding lidar-derived variables in subplot j (j=1...m_i), nested within the i-th plot, the MEM framework for estimating biomass increment in the jth subplot nested within the i-th plot (ΔAGB_{ij}) can be formalized as (after Pinheiro and Bates. 2000 p. 58):

$$\Delta AGB_{ij} = X_{ij}\beta + Z_{ij}b_i + \varepsilon_{ij} \qquad (6)$$

Where:

- b_i is a vector of plot-level random effects;
- X_{ij} and Z_{ij} are *fixed-effects* and *random-effects* regressor matrices;
- ε_{ij} is the within plot error vector that is assumed to be independent between plots and normally distributed;
- and other symbols are as previously defined.

After examining the between plot variability of random coefficients introduced into the base equations, we concluded that a plot-level random effect was necessary. The nlme function (R Development Core Team 2011) was used in this analysis and the enhanced equations had the following general forms.

Model 4: Mixed models for differences between the 2009 and 2004 lidar-derived biomass predictions Equations (7) to (8) have the same fixed components as Eq. (1) and (2) with plot-level random intercepts. The ΔAGB of the j-th subplot from the i-th plot is modeled as:

$$Y4m_{ij} = e^{(\beta_0+bi)+\beta_1 LCH904_{ij}+\beta_2 PCVR4_{ij}} + \varepsilon_{ij} \qquad (7)$$

$$Y9m_{ij} = e^{(\beta_0+bi)+\beta_1 LCH909_{ij}+\beta_2 PCVR9_{ij}} + \varepsilon_{ij} \qquad (8)$$

$$\Delta\widehat{AGB}_{ij} = \hat{Y}9m_{ij} - \hat{Y}4m_{ij} \qquad (9)$$

The fixed effects parts of the model are $\beta_1 LCH904 + \beta_2 PCVR4$ and $\beta_1 LCH909 + \beta_2 PCVR9$ for Equations (7) to (8), with random coefficients $b_i \sim N\left(0, \sigma_b^2\right)$, $\varepsilon_{ij} \sim N\left(0, \sigma_{\varepsilon}^2\right)$ plot-level random effects, and σ_{ε}^2 is the plot-level residual variance. Note that $\hat{Y}9m_{ij}$ and $\hat{Y}4m_{ij}$ are biomass (kg) predictions in 2009 and in 2004.

This model has the same number of fixed coefficients as Equation (1). However, the variation in b_i reflects the variation between plots. The plot-level random effect b_i is assumed to be uncorrelated among plots.

Model 5: Mixed model using differences derived from successive lidar metrics By modeling plot as a random effect, we can explore plot-specific biomass differences in the relationships between biomass increment and changes in lidar metrics. Suppose we observe biomass increment and coinciding lidar metrics change in subplot j ($j = 1 \ldots 4$), nested within the i-th plot. y_{ij} is observed biomass increment in the j-th subplot nested within the i-th plot.

$$\Delta\widehat{AGB}_{ij} = e^{\beta_0 + b_i + \beta_1 \Delta LCH30_{ij} + \beta_2 \Delta PCVR_{ij}} + \varepsilon_{ij} \quad (10)$$

Where:

- b_i is plot-level random effects;
- $b_i \sim \left(0, \sigma_b^2\right)$;
- and σ_ε^2 is the within plot residual variance;
- and all other symbols are as previously defined.

Model 6: Mixed model on differences derived from successive biomass predictions In this approach, ΔAGB is estimated using successive lidar-based biomass predictions that are adjusted with ordinary least squares (OLS) corrections (Draper and Smith 1998, p. 225) and with a random intercept to account for site differences.

$$\widehat{AGB}_{ij} = b_i + \beta_1 \left(\hat{Y}9m_{ij} - \hat{Y}4m_{ij}\right) + \varepsilon_{ij} \quad (11)$$

Where all the symbols are as previously defined.

While Models 2 and 5 use differences in selected lidar metrics between two acquisitions to predict ΔAGB, Models 1, 3, 4, and 6 adjust the differences between the 2009 and 2004 biomass prediction to predict ΔAGB. Lohr (1999, p. 77) refers to the latter approaches as *difference estimation*.

Nonlinear model parameters were estimated using non-linear least squares procedure using the nls function in R software (R Development Core Team 2011). Initial approximations for each parameter were obtained from linear transformation of the equations, where possible. The starting value of each parameter was varied in order to find a global minimum, and the run with the smallest MSE was chosen as providing the final parameter estimates. Residual plots for the base models showed no obvious patterns. As a result, the three fixed-effect nonlinear models were fit assuming a constant residual variance. Mixed models were fit using the nlme function in R (R Development Core Team 2011).

2.5 Model Comparison and Selection The data show considerable variation in lidar-derived attributes among subplots. To retain this variation and include their influence in predicting ΔAGB the predictive performance of the eight equations was evaluated by using leave-one-out cross-validation, where one subplot was excluded from the data and its value was predicted from the remaining n-1 observations using the six prediction strategies. This procedure was repeated for all subplots to calculate the mean difference between predicted and observed values (often called bias) and the root mean squared error (square root of the mean squared difference; RMSE; Rawlings et al. 1998, p. 444). Both RMSE and bias were expressed as percent of the observed mean ΔAGB.

Bias

$$Bias\% = \frac{\sum_{i=1}^{n}\sum_{j=1}^{m_i}\left(\Delta AGB_{ij} - \Delta\widehat{AGB}_{ij}\right)}{n \times \Delta\overline{AGB}} \times 100$$

Where:

- $\Delta\overline{AGB}$ is mean five year biomass increment; and
- AGB_{ij} and $\widehat{AGB}_{ij}$ are observed and predicted five year biomass increments of jth subplot in the ith plot (cluster);
- and all other symbols are as previously defined.

Relative Root Mean Square Error (RRMSE)

$$RRMSE\% = \frac{\sqrt{\sum_{i=1}^{n}\sum_{j=1}^{m_i}\left(\Delta AGB_{ij} - \Delta\widehat{AGB}_{ij}\right)^2}}{n^2 \times \overline{AGB}} \times 100$$

Where all symbols are as previously defined. All statistical analyses were performed in R (R Development Core Team 2011).

3 Results and Discussion

The 2004 and 2009 lidar metrics were strongly correlated with AGB estimated for each year (Table 3). This is consistent with the findings of many other studies (Nilsson, 1996; Næsset, 2002; Næsset, and Bjerknes, 2001; Næsset and Økland, 2002; Popescu et al, 2002; Naesset et al. 2005, Breidenbach *et al* 2007, Goerndt et al. 2010), which found strong and positive relationships between lidar and ground-based biomass predictions.

Correlations between ΔAGB and lidar canopy metrics ranged from 0.51 to 0.56, while correlations between the ΔAGB and ΔLCH and ΔPCVR ranged from 0.31

Table 3: Correlation coefficient matrix for the ground and lidar data sets.

Variable	LCH604	LCH904	PCVR4	LCHCV4	LCH609	LCH909	PCVR9	LCHCV4	Y4	Y9	BI	LCH30	LCH60	LCH90
LCH904	0.97													
PCVR4	0.42	0.43												
LCHCV4	-0.39	-0.19	-0.21											
LCH609	0.97	0.96	0.52	-0.33										
LCH909	0.95	0.99	0.50	-0.21	0.98									
PCVR9	0.56	0.60	0.94	-0.16	0.66	0.66								
LCHCV4	-0.52	-0.37	-0.41	0.88	-0.51	-0.39	-0.39							
Y4	0.73	0.77	0.49	-0.01	0.82	0.80	0.64	-0.24						
Y9	0.73	0.78	0.48	-0.02	0.82	0.81	0.64	-0.24	0.91					
BI	0.55	0.51	0.23	-0.27	0.55	0.51	0.33	-0.35	0.46	0.49				
LCH30	0.35	0.40	0.24	0.14	0.48	0.42	0.38	-0.06	0.69	0.68	0.31			
LCH60	0.31	0.41	0.24	0.22	0.44	0.45	0.40	0.02	0.65	0.65	0.36	0.87		
LCH90	-0.11	-0.05	-0.23	0.14	-0.11	-0.08	-0.12	0.21	-0.03	0.01	0.38	0.19	0.41	
PCVR	0.64	0.72	0.64	-0.06	0.72	0.75	0.87	-0.28	0.72	0.73	0.39	0.49	0.56	0.07

to 0.39 (Table 3). ΔAGB was negatively correlated with LCHCV4 and LCHCV9, but positively correlated with other lidar metrics considered in this study. Of the lidar metrics, LCH604 and LCH609 had the highest correlations with ΔAGB (Table 3). The strengths of these correlations provide some insight into the relationship between lidar attributes and ΔAGB. _

Figures 3a and 3b depict a nonlinear relationship between AGB and selected lidar metrics in 2004 and 2009. Plots of ΔAGB and differences in lidar metrics (i.e., ΔLCH and ΔPCVR) also showed nonlinear relationships (Figures 4a and 4b). The differences in successive lidar metrics were significant covariates in estimating ΔAGB. There were no correlations sufficiently high among covariates to cause problems with collinearity.

3.1 Comparison of Strategies Substantial differences were found among the predictive abilities of the six models examined for predicting ΔAGB (Table 4). Biases for the base models ranged from -1.73 to 2.6%, while for the expanded model bias ranged from -10.4 to 2.97%. The biases of the base models were negligible, while the biases of the enhanced models were high. The higher bias might be attributed to the small sample size that represent a highly varying lidar and ground data that spanned a wide range of elevation (30.4 to 457.2 m), and the use of nonlinear mixed effect model, which are known to be biased without sample calibration data in the leave-one-out validation process (Monelon 2003 and Temesgen et al 2008).

In terms of RRMSE, substantial differences were found among the predictive abilities of the six models examined for estimating ΔAGB. RRMSE for the base models ranged from 95.9 to 196%, while for the enhanced model RRMSE ranged from 76.9 to 136%. Low precision (high RRMSE %) for Models 1, 3, 4, and 6 might be attributed to the difference estimation method these models employed. Lohr (1999, p. 77) asserts that difference estimation works best if the over and under predictions are equally divided and if the sample size is large so that the sampling distribution of the differences would be approximately normal.

In this study, we have found that biomass increment estimation is not as straightforward as it is for biomass yield estimation (Figure 3 vs. Figures 4 and 5). For example, if the average value of ΔAGB is used as predicted value for all plots (no model), the RRMSE would be 110%, which appears a better option than Models 1 and 4. We attribute the relatively poor performance of the ΔAGB models to two factors. First, measurement error resulted because of a time lag of up to five years between ground data and lidar acquisition. Parameters are estimated in a MEM framework using repeated ground and lidar data with a time lag between

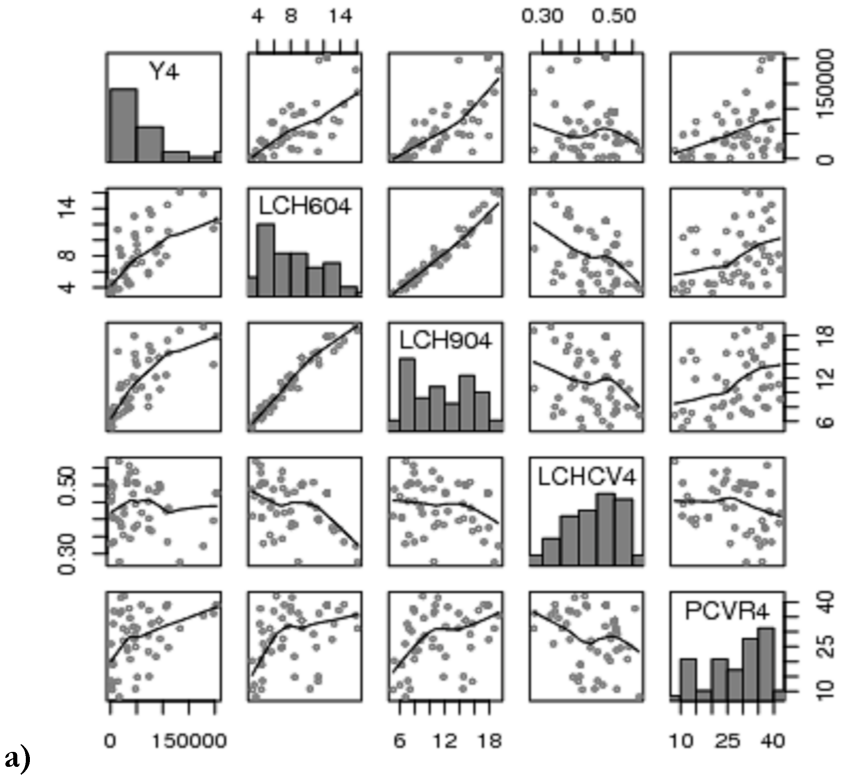

a)

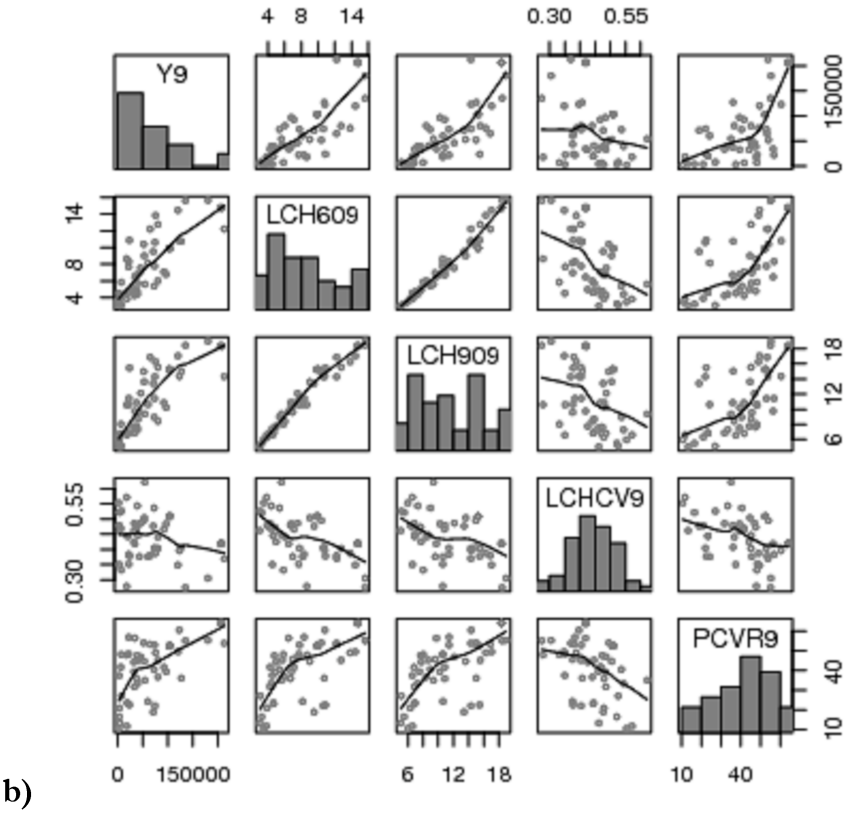

b)

Figure 3: Relationship between above ground biomass (Y4 and Y9), lidar canopy height (LCH) and coefficient of variation (LCHCV) in 2004 (a) and 2009 (b). Note: line indicates locally weighted smoothing line (loess smoother).

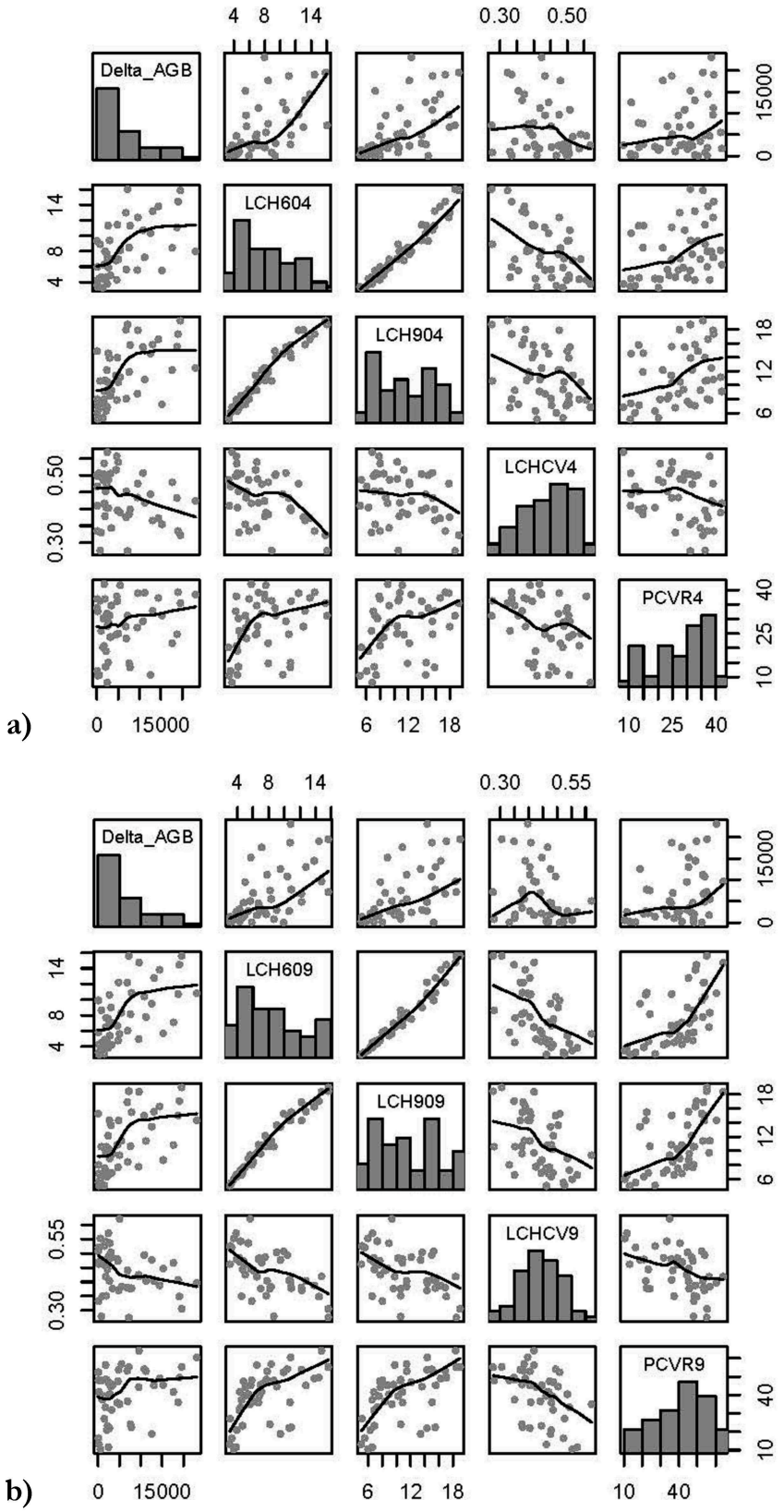

Figure 4: Relationship between biomass increment (Delta_AGB) and lidar canopy height (LCH) and coefficient of variation (LCHCV) in 2004 (a) and 2009 (b). Note: line indicates locally weighted smoothing line (loess smoother).

Table 4: Average bias and relative ΔAGB root mean square error (RRMSE) by fitting strategies.

Model	Bias (%)	Relative RRMSE (%)
Model 1: Using differences between the 2009 and 2004 lidar-derived biomass predictions	2.60	196.0
Model 2: Estimating BI using differences in lidar attributes	1.01	95.9
Model 3: Using differences derived from successive lidar based biomass predictions	-1.73	104.0
Model 4: Mixed models: differences between 2009 & 2004 lidar-based biomass predictions	2.97	136.0
Model 5: Mixed model using differences derived from successive lidar metrics	-10.40	76.9
Model 6: Mixed model on differences derived from successive biomass predictions	-3.80	89.6

and ground measurement and lidar acquisition. This difference can cause problems when trying to estimate covariances of the random error because the covariance structure that is appropriate for the first measurement may not be appropriate for the second set of measurement. Second, differences in species composition, disturbance regimes, and other site-related characteristics are not included in the models while they contribute to the high variation of ΔAGB (96.1 % coefficient of variation).

Improvement in prediction was obtained by using ordinary least square correction factor (i.e., comparing Model 3 with 104% RRMSE to Model 1 with 196% RRMSE and Model 4 with 136% RRMSE to Model 6 with 89.6% RRMSE). Results show that for Model 2, the cross validation RRMSE of the base model form was 95.9% (Table 4). The enhanced Model 5, which included the plot-level random effect, decreased the RRMSE to 76.9%. However, the bias was large (-10.4%) for this model.

Model 5 reduced the predicted root mean square error by 60.8% compared to predictions from the widely used approach, and was selected for future use. The differences in successive lidar-derived canopy attributes can also be used as proxy for estimating ΔAGB under both Model 2 and 5. Canopy structure mimicked via lidar-derived canopy height and density metrics reflect the integrated influence of age, species, disturbance, and site productivity, and is therefore an important and powerful unifying variable.

3.2 Mixed effect analysis Results suggest that there is sizable gain by including plot-level random effect to the base biomass yield and increment equations. According to the fit statistics, all of the mixed effects models were superior to the without the plot effects (Table 4). Compared to the base models, the mixed-effects models had more precise predictions (lower RMSE), but higher bias. Under the mixed model analysis, the alternative models reduced RMSE by an average of 19.8 % for plots with field measured biomass observations. One explanation for the improvement in precision of the enhanced models over the base is that the base models ignore the clustered structure of the data, assuming all subplots are independent, while the enhanced models acknowledge this structure of the data which allows greater flexibility to describe the variance and covariance structure and account for the within and between plot ΔAGB-lidar metrics variation.

Both the mixed-effect model and model without the random effects were compared. When only the fixed component of Model 5 was used the RRMSE was 95.2%. When the MEM used the predicted plot-level random effect, the RRMSE decreased to 76.9%. The mixed-effects model more closely followed the actual values for most plots and indicated that mixed effects model described the ΔAGB-lidar metrics relationship well (Figure 5). This result seems to suggest that incorporating a random effect is a very effective way to consider stand effects. Many of the variables that could influence the ΔAGB-lidar metrics relationship may not be known or may not be practical to measure.

The size of biomass increment was related to subplot-level lidar-derived variables, but varied widely. However, it is unlikely that the relationships of ΔAGB and the lidar covariates have a constant relationship over the study area. Motivated by the hierarchical structure of the data, we addressed the plot-level variation with a random coefficient model. Under the mixed model analysis, residual plots indicated a constant relationship across lidar canopy height and percent canopy cover return gradients.

Mixed effect models are effective statistical tools, but it should also be recognized that their effective application requires some sample growth data. As such, the need for sample data limits their applications. If a subsample of ground data is available to predict the plot random intercept, the enhanced model is suggested. In the absence of ground data, the plot-level random effect is usually set to zero and the model without the plot effects is used. Using a mixed-effects model in this case can result in a substantial decrease in predictive performance, but the bias will increase (Monelon 2003

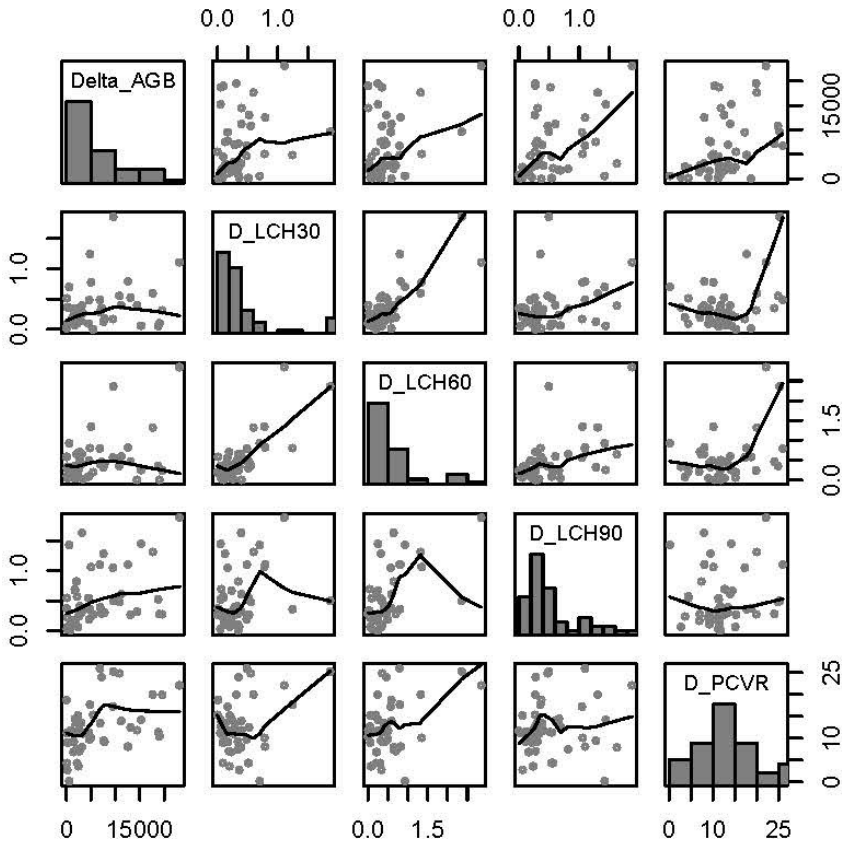

Figure 5: Relationship between biomass increment (Delta_AGB) and differences in selected lidar metrics. Note: line indicates locally weighted smoothing line (loess smoother).

and Temesgen et al 2008). In which case, we would not recommend the use of mixed effect model when a subsample of ΔAGB is not available. Instead, Model 2 with only the fixed effect parameter is suggested (Table 5).

3.3 Final Parameter Estimates Among the base models forms, Model 2 had the lowest cross-validation RMSE. It reduced the predicted RRMSE by 51.2% compared to Model 1. The enhanced counter model (Model 5) which included random intercept resulted in a decrease of RMSE by 19.8% while its bias increased. Table 5 shows the estimated parameters and associated standard errors for Models 2 and 5.

Residual plots for both models showed no obvious patterns. Based on the residual plots above, it appears that there is not a problematic level of variance heterogeneity. Also, residuals do not show any clear pattern with the lidar-derived variables included in the model, indicating the assumption of independent error is justified.

Scatter plots of residuals were constructed for the fixed parts and the random part of Model 5 (Figure 6). The scatter plots of the mixed-effects model showed more homogeneous residual variance over the full range of the predicted values and no systematic pattern in the variation of the residuals. It indicates that the fixed-effect models improve the model performance compared to the model without the random effects.

4 Concluding Remarks

Regression-based methods for predicting forest inventory variables using lidar-derived canopy height and density metrics have been well described and demonstrated in the research literature (Næsset et al. 2005, Goerndt et al. 2010). Less well developed, however, are reliable techniques for estimating ΔAGB. In this study, we have shown that biomass increment estimation is not as straightforward as it is for biomass yield estimation (Figure 3 vs. Figures 4 and 5).

There was a strong relationship between total estimated biomass and lidar metrics for both measurement periods. Our results are consistent with previous studies, which found that ΔAGB values are extremely variable within an eco-region, and a portion of this variability can be explained by the location of plots over the

Table 5: Estimated parameters and associated standard errors for model the selected to estimate biomass increment.

Model 2			Model 5		
Coefficient	Estimate	Standard Error	Coefficient	Estimate	Standard Error
β_0	8.0242	0.3745	β_0	7.79	0.344
β_1	0.0441	0.1597	β_1	0.14	0.171
β_2	0.0478	0.0214	β_2	0.07	0.02
			σ_e	3426	
			σ_b	0.63	

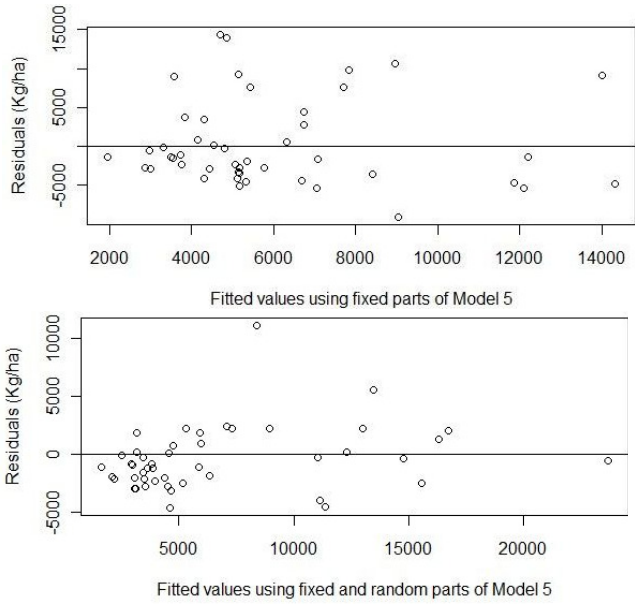

Figure 6: Scatter plot of residuals versus fitted values using the fixed parts (a) and random part (b) of the mixed effect of Model 5.

land base. Developing models that relate ΔAGB to lidar metrics is an important step forward for forest monitoring and biomass assessment. Recognizing this fact, this analysis represents one of the first attempts to develop ΔAGB equations for coastal Alaska forests and relate ΔAGB to selected lidar metrics.

Despite lack of a definitive relationship between ΔAGB and successive lidar metrics, the results of this study indicate that repeated lidar measurements can be used to estimate ΔAGB and monitor change over time. Yet, additional research is warranted to improve our understanding of the relationships between the distribution of lidar measurements and ΔAGB in Coastal Alaska forests.

The following recommendations may improve biomass increment model fit and performance for future lidar surveys: (1) ground-reference samples and remotely sensed data should be ideally collected in the same year and preferably during the same part of the growing season to eliminate discrepancies induced by growth, mortality, disturbance, or phenology; and (2) maximize the number of ground-samples collected and improve model specification by including climate and site explanatory variables and by exploring other modeling strategies that account for complex interactions among predictors; and (3) use large plot footprint sizes to minimize spatial co-registration error between lidar and field measurements or use systems that allow precise positioning.

Moreover, if biomass increment were studied over a longer temporal scale the amount of biomass increment might exceed the errors associated with its estimation, thereby allowing it to be successfully and more accurately detected by the lidar. Future biomass increment studies would benefit enormously from further investigation into the quantitative effects of different spatial and temporal resolutions.

Acknowledgements

We thank Dr. Jeremy Groom for his insights and comments on an earlier draft. We gratefully acknowledge the Editor and three anonymous reviewers for their helpful comments and insights on an earlier version of the manuscript. We thank the Pacific Northwest Research Station for providing data and financial support.

References

Andersen, H.-E., R.J. McGaughey, and S.E. Reutebuch. 2005. Estimating forest canopy fuel parameters using LIDAR data. Remote Sensing of Environment. 94: 441-445.

Andersen, H. E., T. Clarkin, K. Winterberger, and J. Strunk. 2009. An accuracy assessment of positions obtained using survey- and recreational-grade global positioning system receivers across a range of forest conditions within the Tanana Valley of interior Alaska. Western Journal of Applied Forestry. 24: 128-136

Andersen, H.-E., J. Strunk, and H. Temesgen. 2011. Using airborne lidar as a sampling tool for estimating

forest biomass resources in the upper Tanana Valley of interior Alaska. Western Journal of Applied Forestry. 109: 371-377.

Baker, J.S., B.A. McCarl, B.C. Murray, S.K. Rose, R.J. Alig, D. Adams, G. Latta, R. Beach, and A. Daigneault. 2010. Net farm income and land use under a U.S. greenhouse gas cap and trade. Policy Issues (P. 17) 7:1-5

Balzter, H., L. Skinner, A. Luckman, and R. Brooke. 2003. Estimation of tree growth in a conifer plantation over 19 years from multi-satellite L-band SAR. Remote Sensing of Environment. 84: 184–191.

Bollandsås, O. M. and E. Naesset. 2010. Using delta values of multi-temporal first-return small footprint airborne laser scanner data to predict change of tree biomass in mountain spruce forests. Silvilaser 2010 proceedings, September 14th - 17th, Freiburg, Germany.

Bollandsås, O. M., T. Gregoire, E. Næsset, and B. H. Øyen, 2013.Detection of biomass change in a Norwegian mountain forest area using small footprint airborne laser scanner data. Statistical Methods & Applications. 22: 113-129

Breidenbach, J., R.J. McGaughey, H.-E. Andersen, G. Kändler, and S.E. Reutebach. 2007. A mixed effects model to estimate stand volume by means of small footprint airborne lidar data for an American and a German study site. In: Rönnholm, P., Hyyppä, H. and Hyyppä, J. (eds.). Proceedings of ISPRS Workshop Laser Scanning 2007 and Silvilaser 2007, September 12–14, 2007, Finland. International Archives of Photogrammetry, Remote Sensing and Spatial Information Sciences XXXVI(Part 3/W52). p. 77–83.

Breidenbach, J., E. Kublin, R. McGaughey, H.-E. Andersen, and S.E. Reutebuch. 2008. Mixed-effects models for estimating stand volume by means of small footprint airborne laser scanner data. Photogrammetric Journal of Finland. 21: 4-15.

Cairns, M.A., I. Olmsted, J. Granados, and J. Argaez. 2003. Composition and aboveground tree biomass of a dry semi-evergreen forest on Mexico's Yucatan Peninsula. For. Ecol. and Mgmt. 186: 125-132.

Carroll, R.J., D. Ruppert, L.A. Stefanski, and C. Crainiceanu. 2006. Measurement error in nonlinear models. A modern perspective, 2nd ed. Chapman and Hall.

Diggle, P., P. Heagerty, K.Y. Liang, and S. Zeger. 2002. Analysis of longitudinal data. 2nd ed. Oxford Press, Oxford.

Donoghue, D.N.M., P.J. Watt, N.J. Cox, R.W. Dunford, J. Wilson, S. Stables, and S. Smith. 2004. An evaluation of the use of satellite data for monitoring early development of young Sitka spruce plantation forest growth. Forestry. 77: 383–396.

Edmons, R.L., K.K. Agee, and R.I. Gara. 2000. Forest health and protection. McGraw-Hill, 630 pp.

Fitzmaurice, G., M. Davidian, G. Molenberghs, and G. Verbeke. 2008. Longitudinal data analysis. Boca Raton, Florida, Chapman & Hall/CRC.

Goerndt, M.E., V.J. Monleon, and H. Temesgen. 2010. Relating forest attributes with area- and tree-based Lidar metrics for western Oregon. Western Journal of Applied Forestry. 25: 105-111.

Gough, C.M., C.S. Vogel, H.P. Schmid, and P.S. Curtis. 2008. Controls on annual carbon storage: lessons from the past and predictions for the future. BioScience. 58:7:609-622.

Goldfield, S.M. and R.E. Quandt. 1965. Some tests for homoscedasticity. J. Amer. Stat. Assn. 60: 539-547.

Gregoire, T. G. 1987. Generalized error structure for forestry yield models. Forest Science. 33: 423-444.

Hall, D.B. and R.L. Bailey. 2001. Modeling and prediction of forest growth variables based on multilevel nonlinear mixed models. Forest Science. 47: 311–321.

Hazard, J.H., H. Schreuder, and V. LaBau. 1995. The Alaska four-phase forest inventory sampling design using remote sensing and ground sampling. Photogrammetric Engineering and Remote Sensing. 61(3): 291 - 302.

Hudak, A. T., E. K. Strand, L. A. Vierling, J.C. Byrne, J. U. H Eitel,.S. Martinuzzi, and M.J. Falkowski. 2012. Quantifying aboveground forest carbon pools and fluxes from repeat LiDAR surveys. Remote Sensing of Environment. 123:25-40.

Hyde, P., R. Dubayaha, W. Walker, J. Bryan Blair, M. Hofton and C. Hunsaker. 2006. Mapping forest structure for wildlife habitat analysis using multisensor (Lidar, SAR/InSAR, ETM+, Quickbird). Remote Sensing of Environment. 120: 63-73.

Lohr, S.L. 1999. Sampling: Design and Analysis. Duxbury, Pacific Grove, CA. 494 p.

Ming, S.X. and S. Huang. 2010. Incorporating correlated error structures into mixed forest growth models: prediction and inference implications. Can. J. For. Res. 40(5): 977-990.

Monleon, V.J. 2003. A hierarchical linear model for tree height prediction. *In*: Proceedings of the 2003 meeting of the American Statistical Association, Section on Statistics and the Environment. Alexandria, VA p. 2865-2869.

Meyer, V. S.S. Saatchi, J.Chave, J.W.Dalling, S.Bohlman, G.A.Fricker, C.Robinson, M.Neumann, and S.Hubbell, 2013. Detecting tropical forest biomass dynamics from repeated airborne lidar measurements. Biogeosciences. 10: 5421-5438.

McRoberts, R.E., O. M. Bollandsås, and E. Næsset. 2014. Modeling and estimating change. In. M. Maltamo et al. (eds.), Forestry Applications of Airborne Laser Scanning: Concepts and Case Studies. Managing Forest Ecosystems. Springer. Pp. 269-293.

Næsset, E., O. M. Bollandsås, T. Gobakken, T. Gregoire, and G. Ståhl. 2013. Model-assisted estimation of change in forest biomass over an 11 year period in a sample survey supported by airborne LiDAR: A case study with post-stratification to provide "activity data". Remote Sensing of Environment. 128: 299-314.

Næsset, E., T. Gobakken, J. Holmgren, H. Hyyppä, J. Hyyppä, and M. Maltamo 2004. Laser scanning of forest resources: The Nordic experience. Scandinavian Journal of Forest Research. 19: 482–499

Næsset, E. and T. Gobakken. 2005. Estimating forest growth using canopy metrics derived from airborne laser scanner data. Remote Sensing of Environment. 96: 453–465.

Neter, J., W. Wasserman, and M.H. Kutner. 1990. Applied linear regression models. Richard D. Irwin. Boston. 1181 pp.

Pinheiro, J.C. and D. M. Bates. 2000. Mixed effects models in S and S-plus. Springer, New York, 528 pp.

R Development Core Team. 2011. R: a language and environment for statistical computing. R Foundation for Statistical Computing, Vienna, Austria. Available at http://www.R-project.org.

Roesch, F.A. and G.A. Reams. 1999. Analytical alternatives for an annual inventory system. Journal of Forestry. 97: 44-48.

Ståhl, G., H. Sören, T. Gregoire, T. Gobakken, E. Næsset, and R. Nelson.2011. Model-based inference for biomass estimation in a LiDAR sample survey in Hedmark County, Norway. Can. J. For. Res. 41: 96-107.

Temesgen, H., V.J. Monleon, and D.W. Hann. 2008. Analysis of nonlinear tree height prediction strategies for Douglas-fir forests. Can. J. For. Res. 38: 553-565.

Temesgen, H., M.E. Goerndt, G. P. Johnson, D.M. Adams, and R.A. Monserud. 2007. Forest measurement and biometrics in forest management: status and future needs of the Pacific Northwest USA. Journal of Forestry. 105: 233-238.

Yarie, J., E. Kane, and M. Mack. 2007. Aboveground biomass equations for the trees of interior Alaska. Agricultural and Forestry Experiment Station Bulletin: 115. University of Alaska-Fairbanks. 15 p.

Yu, X., J. Hyyppa, H. Kaartinen, and M. Maltamo. 2004. Automatic detection of harvested trees and determination of forest growth using airborne laser scanning. Remote Sensing of Environment. 90: 451–462.

Yu, X., J. Hyyppa, A. Kukko, M. Maltamo, and H. Kaartinen. 2006. Change detection techniques for canopy height growth measurements using airborne laser scanner data. Photogrammetric Engineering and Remote Sensing. 72: 1339–1348.

van Hees, W.W.S. 2005. Spruce reproduction dynamics on Alaska's Kenai Peninsula, 1987-2000. United States Department of Agriculture Forest Service Pacific Northwest Research Station Research Paper PNW-RP-563.